Accepted Manuscript

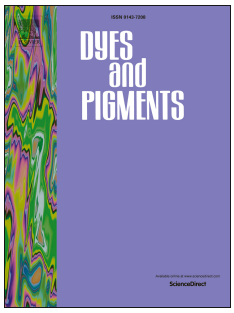

A 1,8-naphthalimide-based chemosensor with an off-on fluorescence and lifetime imaging response for intracellular Cr^{3+} and further for S^{2-}

Mingming Yu, Weiwei Du, Wan Zhou, Haixia Li, Chunxia Liu, Liuhe Wei, Zhanxian Li, Hongyan Zhang

PII: S0143-7208(15)00488-X

DOI: 10.1016/j.dyepig.2015.12.001

Reference: DYPI 5024

To appear in: *Dyes and Pigments*

Received Date: 18 August 2015

Revised Date: 28 November 2015

Accepted Date: 1 December 2015

Please cite this article as: Yu M, Du W, Zhou W, Li H, Liu C, Wei L, Li Z, Zhang H, A 1,8-naphthalimide-based chemosensor with an off-on fluorescence and lifetime imaging response for intracellular Cr^{3+} and further for S^{2-}, *Dyes and Pigments* (2016), doi: 10.1016/j.dyepig.2015.12.001.

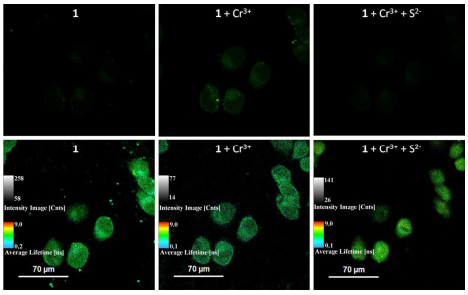

Graphical Abstract

The fluorescence and lifetime change of the chemosensor and the '*in situ*' prepared Cr^{3+} complex upon addition of Cr^{3+} and S^{2-} on test paper and in living cells have been successfully demonstrated.

A 1,8-naphthalimide-based chemosensor with an off-on fluorescence and lifetime imaging response for intracellular Cr^{3+} and further for S^{2-}

Mingming Yu[a,*], Weiwei Du[a], Wan Zhou[a], Haixia Li[a], Chunxia Liu[a], Liuhe Wei[a], Zhanxian Li[a,*], Hongyan Zhang[b,*]

* Corresponding author.

a. College of Chemistry and Molecular Engineering, Zhengzhou University, Zhengzhou, 450001, China.

E-mail address: yumm@zzu.edu.cn (M. Yu), lizx@zzu.edu.cn (Z. Li).

Tel: +(86)371-67781205

Fax: +(86)371-67781205

b. Key Laboratory of Photochemical Conversion and Optoelectronic Materials, Technical Institute of Physics and Chemistry, Chinese Academy of Sciences, Beijing, 100190, China

E-mail address: zhanghongyan@mail.ipc.ac.cn (H. Zhang).

Abstract

A novel 1,8-naphthalimide-based chemosensor was designed and synthesized for rapid recognition of Cr^{3+}. The desired sensor showed off-on fluorescent and lifetime-based response upon Cr^{3+} and S^{2-} in solution, on test paper and in cells. With the intensity-based method, the limit of quantification (LOQ) value was 0–5.5 × 10^{-5} M and the detection limit could be as low as 0.60 ppm. The '*in situ*' prepared Cr^{3+} complex can recognize S^{2-} among a series of common anions with high selectivity and sensitivity, the LOD can be as low as 307 nM. The lifetime of the sensor changes from 4.95 to 4.89 and further to 5.88 ns upon addition of Cr^{3+} and S^{2-} in turn.

Keywords: Sensor; Off-on fluorescence; Fluorescence lifetime imaging microscopy; FLIM; Cr^{3+} ion; S^{2-} anion

1. Introduction

In recent years, great achievement has been achieved in the development of fluorescent chemosensors toward environmentally and biologically important species such as metal ions and anions due to several advantages over other methods such as high sensitivity, specificity, and real-time monitoring with fast response [1−5]. Triple-charged metal cation detection is of significance owing to its crucial influence in a wide range of environmental and human health areas [6−8]. As a significant essential trace element in biological systems, trivalent chromium (Cr^{3+}) is an important component of glucose tolerance factor, enhancing the biological function of insulin to promote the absorption of glucose; Cr^{3+} can inhibit cholesterol biosynthesis which affects lipid metabolism process. Cr^{3+} deficiency can cause diabetes, atherosclerosis, and growth retardation [9−10], whereas excessive chromium can cause genotoxic effects [11]. Cr^{3+} has been proven to nonspecifically bind to DNA and other cellular components resulting in inhibition of transcription and possibly DNA replication [12]. In addition, as an environmental contaminant and due to various industrial and agricultural activities, the build-up of Cr^{3+} especially in food and water is a matter of concern [13,14]. Besides, sulfide anions are widely used in many fields, such as the production of sulfur and sulfuric acid, dyes and cosmetic manufacturing [15]. It also exists in biosystems because of microbial reduction of sulfate by anaerobic bacteria or sulfide generation from the sulfur-containing amino acids in meat proteins [16]. Owing to its toxicity, exposure to a high level of sulfide anions could cause loss of consciousness, irritation of mucous membranes and suffocation [17]. In water, sulfide anions may be in the form of HS^{-}, which becomes even more toxic. High concentration of HS^{-} can result in personal distress, permanent brain damage, unconsciousness, or even asphyxiation [18]. Thus, it is urgent to develop fluorescent chemosensors toward Cr^{3+} and S^{2-}.

It is generally believed that chemosensors with fluorescence enhancement are more efficient than fluorescent "turn-off" based probes [19−25]. However, the paramagnetic nature of Cr^{3+} leads fluorescence quenching of the fluorophore via the enhancement of spin-orbit coupling [26−32], in the last few years, there are only few successful cases of fluorescence enhancement type sensors for Cr^{3+} [33−38], and for S^{2-} [16, 39−45]. Therefore, it is essential to explore new chemosesnors for Cr^{3+} and S^{2-} in biological and environmental samples.

In addition to fluorescence-based sensors, lifetime-based sensors have attracted great attention [46−52]. These sensors provide the information on the analyte through obvious changes in emission lifetimes upon interaction with the analyte. The rapid development of fluorescence lifetime imaging microscopy (FLIM) makes the lifetime-based detection of intracellular analytes possible. In FLIM imaging, luminescence lifetime is measured at each spatially resolvable element of a microscope image [53], and the lifetime obtained is independent of probe concentration and excitation laser intensity [54]. In addition, when long-lived luminescent sensors are employed for FLIM imaging, the signals from the sensors can be distinguished from the autofluorescence [55−57], which typically has a fluorescence lifetime ranging from the picosecond to nanosecond level. As one of the most promising photoresponsive materials, 1,8-naphthalimide-based derivatives have been well recognized for excellent photostability, high fluorescence quantum yields and large Stokes' shift. Moreover, fluorescent characteristics were anticipated to be tuned through judicious structural modifications [58−64]. However, no 1,8-naphthalimide-based fluorescent chemosensors for Cr^{3+} have been reported and the reported S^{2-}-fluorescent sensors are not many. Herein, as illustrated in **Scheme 1**, we synthesized a highly sensitive and stable fluorescent 1,8-naphthalimide-based dye compound **1**, which can quantitatively detect the concentration of Cr^{3+} with dramatically enhanced fluorescence.

The detection limit on fluorescence response of the sensor can be as low as 0.60 ppm. The '*in situ*' prepared Cr^{3+} complex (**1•Cr**) showed high selective recognition of S^{2-} with distinct changes in its fluorescence. The LOD can be as low as 307 nM.

2. Experimental

2.1. Methods and materials

All commercial grade chemicals and solvents were purchased and were used without further purification. Compound **1** was synthesized according to **Scheme 1** [65,66].

(**Insert: Scheme 1**)

Mass spectra were obtained on high resolution mass spectrometer (IonSpec4.7 Tesla FTMS-MALDI/DHB). ^{1}H and ^{13}C NMR spectra were recorded on a Bruker 400 NMR spectrometer. Chemical shifts are reported in parts per million using tetramethylsilane (TMS) as the internal standard.

2.2. Spectral characterizations

All spectral characterizations were carried out in HPLC-grade solvents at 20 °C within a 10 mm quartz cell. Fluorescence spectroscopy was determined on a Hitachi F-4500 spectrometer. The fluorescence quantum yield was measured at 20 °C with quinine bisulfate in 1 M H_2SO_4 (Φ_{fr} = 0.546) selected as the reference [67]. Time-resolved fluorescence spectra were measured on a LifeSpec picosecond TRF spectrometer (Edinburgh Instruments Ltd.).

2.3. Fluorescence and lifetime imaging experiments in living Hela cells

Hela cells were seeded in a 12-well plate in Dulbecco's modified Eagle's medium (DMEM) supplemented with 10% fetal bovine serum and 1% penicillin. The cells were incubated under an atmosphere of 5% CO_2 and 95% air at 37 °C for 24 h before the cell

imaging experiments. The cells were washed three times with PBS buffer before used. The cells were firstly incubated with sensor **1** (10 μM) for 10 min at 37 °C, then incubated with Cr^{3+}(40 μM) for another 5 min and then incubated with S^{2-} (80 μM) for another 2 min.

Fluorescence and lifetime imaging experiments in Living Hela cells were operated with Nikon A1Rmp-PicoQuant FLIM. 405 nm semiconductor laser was used for fluorescence imaging experiments, and LDH-P-C-405B laser was used for lifetime imaging experiments.

*2.4. Synthesis of compound **1***

A mixture of compound **2** (0.2330 g, 0.7 mmol), K_2CO_3 (0.4070 g, 2.8 mmol) and propargyl bromide (0.068 mL, 0.7 mmol) in 15 mL acetonitrile was refluxed for 8 h, then cooled to room temperature, filtered, and the filter cake was washed with acetonitrile for three times. The crude product was obtained from the concentration of the filtrate in vacuum. The final product (0.1946 g) was purified by column chromatography over silica gel column using ethyl acetate/petroleum ether (10:1) as eluent. The yield was 76.5%. Characterization of compound **1**: HRMS (EI) m/z: calcd for $C_{21}H_{21}N_3O_3$ [M + H], 364.1583; found, 364.1664. ^{1}H NMR (400 MHz, $CDCl_3$, TMS): δ_H 8.59 (d, 1H), 8.52 (d, 1H), 8.43 (d, 1H), 7.70 (m, 1H), 7.22 (d, 1H), 4.46 (t, 2H), 3.99 (t, 2H), 3.49 (s, 2H), 3.36 (t, 4H), 2.93 (t, 4H). ^{13}C NMR (100 MHz, $CDCl_3$): δ_C 165.39, 164.95, 132.96, 131.47, 130.66, 129.97, 126.08, 125.72, 122.93, 116.34, 115.03, 62.07, 52.87, 51.77, 46.87 and 42.75.

3. Results and Discussion

*3.1. Fluorescence studies of chemosensor **1** towards Cr^{3+}*

To investigate the changes in fluorescence emission spectrum of **1** upon exposure to

$Cr(NO_3)_3$ (Cr^{3+}), fluorescence titrations were conducted with water solution of Cr^{3+} in aqueous solution of **1** (1.0×10^{-5} M, water/ethanol = 6:4, v/v) (**Fig. 1**). Upon excitation at 385 nm, the fluorescence emission intensity of **1** gradually increased (Φ_{fr} changed from 0.018 to 0.335, I/I_0 = 40) as the concentration of Cr^{3+} increased, indicating an efficient Cr^{3+}-selective fluorescent "off-on" behavior. The increased emission intensity is probably due to the complex of Cr^{3+} and **1**, in which, the coordination of Cr^{3+} and **1** inhibits the photo-induced electron transfer (PET) from electron-donator piperazine moiety to electron-receptor 1,8-naphthalimide moiety.[66] **Fig. S1** (in the Supporting Information) indicates the relationship between the fluorescence peak intensity at 520 nm and the concentration of Cr^{3+}. A good linear relationship between the fluorescence peak at 520 nm and the concentration of Cr^{3+} was obtained at concentration range of 0 and 5.5×10^{-5} M (right of **Fig. 1**), implying that Cr^{3+} can be quantitatively detected at a wide concentration range. According to this linear calibration graph, the detection limit of probe **1** for Cr^{3+} is found to be about 1.68×10^{-6} M (0.60 ppm) based on signal-to-noise ratio (S/N) = 3.[68,69] This result proved that sensor **1** shows high sensitivity to Cr^{3+}. Job's plot indicated that sensor **1** chelates Cr^{3+} with 1:1 stiochiometry (**Fig. S2** in the Supporting Information).

(**Insert: Fig. 1**)

(**Insert: Fig. 2**)

(**Insert: Fig. 3**)

*3.2. Counterion effect on the Cr^{3+}-selective properties of sensor **1***

Experiments to explore the counterion effect on the Cr^{3+}-selective properties of sensor

1 were also performed (**Fig S3** in the Supporting Information). Sulfate and nitrate counteranions had similar influence as chloride, demonstrating that the three kinds of anions do not coordinate the metal ions while compound **1** was interacting with Cr^{3+}. This indicates that compound **1** as a fluorescent sensor has a much wide application range in sensing Cr^{3+} ions.

*3.3. The selectivity and anti-disturbance effect study of sensor **1** for Cr^{3+}*

To evaluate the selectivity of sensor **1** for Cr^{3+}, various metal ions (K^{+}, Ca^{2+}, Na^{+}, Mg^{2+}, Al^{3+}, Co^{2+}, Cr^{3+}, Ni^{2+}, Cu^{2+}, Zn^{2+}, Pb^{2+}, Hg^{2+}, Mn^{2+}, Cd^{2+}) were tested. As shown in **Fig. 2** and black bars of **Fig. 3,** only the introduction of $Cr^{3+}$to the sensor **1** solution induced a significant enhancement in the fluorescent intensity at 520 nm. In the same condition, other tested metal ions mentioned above did not induce any obvious fluorescence enhancement to the sensor **1** solution.

To further assess its utility as a Cr^{3+}-selective fluorescent sensor, its fluorescence spectrum response to Cr^{3+} in the presence of other metal ions mentioned above (red bars of **Fig. 3**) was also tested. The results demonstrated that all of the selected species have no interference in the detection of Cr^{3+}. This result strongly indicates that compound **1** could be an excellent fluorescent sensor towards Cr^{3+} with strong anti- interference ability.

*3.4. pH range of application of **1** toward Cr^{3+}*

For both environmental and biological applications of the fluorescent sensor, it would be much better if the sensing works over a wide range of pH. The right panel of **Fig. S4** in the Supporting Information shows that in aqueous solution the suitable pH range for Cr^{3+} determination is 4-6, where the fluorescence off-on behavior can be operated by Cr^{3+} binding. The short pH application range may be ascribed to the strong protonation ability

of sensor **1**.

*3.5. Reversibility study of the binding of **1** to Cr^{3+}*

To examine the reversibility of the binding of chemosensor **1** to Cr^{3+}, a water solution containing 4 equiv S^{2-} was added to the **1•Cr^{3+}** solution. When S^{2-} was added to the **1•Cr^{3+}** solution, fluorescence signals identical to those of **1** were restored (**Fig S5** in the Supporting Information and **Fig. 4**), demonstrating that Cr^{3+} was removed from the **1•Cr^{3+}** complex by S^{2-}. That is, the binding of **1** and Cr^{3+} is really chemically reversible.

(**Insert: Fig. 4**)

(**Insert: Fig. 5**)

*3.6. Sensing mechanism of **1** to Cr^{3+}*

Reference compound **2** was applied to determine the coordination mode of **1** with Cr^{3+}. Upon addition of different metal ions to the solution of compound 2 respectively, no fluorescence spectra change was observed (**Fig S6** in the Supporting Information), indicating that compound **2** cannot be a fluorescent sensor toward these metals. In addition, the sensing mechanism was confirmed by the ^{1}H NMR titration experiments of compound **1** in 0.5 mL CD_3OD with different amounts of the Cr^{3+} anion (0, 0.5, and 1 equiv). As shown in **Fig S7** in the Supporting Information, upon addition of Cr^{3+}, the four peaks at 3.49, 3.33, 2.95 and 2.80 shifted to low field (3.69, 3.40, 3.16, and 2.98), confirming that the two nitrogen atoms of the piperazine unit and the alkynyl group coordinate the Cr^{3+} anion.

*3.7. Fluorescence sensing properties of the 'in situ' prepared Cr^{3+} complex (**1•Cr^{3+}**) toward S^{2-}*

As we have mentioned above, only the addition of S^{2-} can result in the fluorescence of

the '*in situ*' prepared **1•Cr^{3+}** signals restoring. That is, the complex **1•Cr^{3+}** can detect S^{2-} with fluorescence method.

To investigate the changes in fluorescence spectrum of the complex **1•Cr^{3+}** upon exposure to S^{2-}, fluorescence titration experiments were conducted. As shown in left of **Fig. 4**, upon addition of S^{2-} water solution, fluorescence at 520 nm gradually decreased, implying that Cr^{3+} is removed from the complex **1•Cr^{3+}** by S^{2-}, and the complex **1•Cr^{3+}** can detect S^{2-}. In concentration range of 0 and 530 μM, the fluorescence intensity at 520 nm is in good linear relationship with S^{2-} concentration (right of **Fig. 4**), implying that S^{2-} can be quantitatively detected in a wide concentration range. The LOD value from the fluorescence titration experiment can be as low as 307 nM.

To examine the selectivity and anti-disturbance capacity toward S^{2-}, further experiments were carried out. Upon addition of different anions, only S^{2-} can induce fluorescence at 520 nm of the complex **1•Cr^{3+}** decreasing (black bars of **Fig 5**), other representative anions, such as F^-, Cl^-, Br^-, I^-, CO_3^{2-}, CH_3COO^-, NO_3^-, PO_4^{3-}, NO_2^-, SO_3^{2-}, HSO_3^-, ClO_3^-, N_3^-, SiO_3^{2-}, HCO_3^-, HPO_4^{2-}, $H_2PO_4^-$, SCN^-, and SO_4^{2-} showed almost no effects on the fluorescence of the complex **1•Cr^{3+}**, implying high selectivity of the complex **1•Cr^{3+}** toward S^{2-}. The competition experiments were conducted in the presence of Cr^{3+} and S^{2-} mixed with many anions (F^-, Cl^-, Br^-, I^-, CO_3^{2-}, CH_3COO^-, NO_3^-, PO_4^{3-}, NO_2^-, SO_3^{2-}, HSO_3^-, ClO_3^-, N_3^-, SiO_3^{2-}, HCO_3^-, HPO_4^{2-}, $H_2PO_4^-$, SCN^-, and SO_4^{2-}) respectively (red bars). No significant fluorescence spectra change were found by comparison with that without the other anions, which revealed strong anti-disturbance capacity of the complex **1•Cr^{3+}** toward S^{2-}.

3.8. Application on Test Paper

As shown in the above, chemosensor **1** can detect Cr^{3+} in aqueous solution, it inspired

us to further investigate the feasibility of solid materials for point-of-care detection application. Test paper was selected and the fluorescence detection properties were studied by a UV lamp with photography as well as solid fluorescence spectroscope. In the detection process, the sensor spots were prepared by dropping 5 μL 10 μMsolutions of **1** $Cr(NO_3)_3Cr^{3+}$portable ultraviolet lamp. As shown in **Fig. 6**, the sensor spots emitted bright blue-green fluorescence upon the addition of Cr^{3+} under UV illumination, meanwhile an enhancement of the fluorescence intensity at 495 nm could be recorded. Additionally, the sensor spots emitted fluorescence only upon the addition of Cr^{3+} (**Fig. 7**), demonstrating the high selectivity of sensor **1** as solid materials toward Cr^{3+}.

(**Insert: Fig. 6**)

(**Insert: Fig. 7**)

*3.9. Application of Sensor **1** in Cellular Imaging*

The practical utility of using sensor **1** to detect Cr^{3+} and further S^{2-} in an imagewise manner within living Hela cells was explored (**Fig. 8**). When Hela cells were incubated with 10 μM probe **1** only for 10 min at 37 °C, no obvious fluorescence was observed (f of **Fig. 8**). However, when Hela cells were preincubated with Cr^{3+} (40 μM) and then incubated with probe **1** (10 μM) for 5 min, a significant green fluorescence inside the cells was observed with the aid of an inverted fluorescence microscope (g of **Fig.8**), implying that the stimulation of Cr^{3+} toward probe **1** only for 5 min can give green emission. Furthermore, when Hela cells were preincubated with Cr^{3+} (40 μM), probe **1** (10 μM), and then incubated with 80 μM S^{2-} for 2 min, no obvious fluorescence was also observed (h of **Fig. 8**), implying that addition of S^{2-} lead to the fluorescence quenching of the complex **1•Cr^{3+}**. Bright-field measurements indicated that the cells before and after addition of $Cr^{3+}$and S^{2-} remained viable throughout the imaging experiments (a, b, c, and

d of **Fig. 8**). Thus, probe **1** is capable of permeating into cells and sensing Cr^{3+} and S^{2-} in living cells.

Lifetime-based detection of Cr^{3+} and S^{2-} was conducted in FLIM imaging. As shown in **Fig. 9**, cells treated with 10 μM sensor **1** for 2 h at 37 °C displayed a relatively short lifetime of 4.89 ns. When 40 μM Cr^{3+} was added in the growth media, the lifetime of microregions hardly changed (4.95 ns)**.** A lifetime of 5.88 ns was obtained for the above system upon addition of 80 μM S^{2-}**.** FLIM imaging result demonstrates that S^{2-} cannot release Cr^{3+} from the complex, and the possible case is that S^{2-} take the place of chloride ion to coordinate Cr^{3+}. This result implied that he '*in situ*' prepared **1•Cr^{3+}** complex was able to serve as a Lifetime-based sensor for S^{2-}.

(**Insert: Fig. 8**)

(**Insert: Fig. 9**)

4. Conclusion

In summary, a Cr^{3+} selective fluorescent "off-on" and lifetime-based chemosensor 1,8-naphthalimide derivative **1** was synthesized, which displays a high selectivity, antidisturbance for Cr^{3+} among environmentally and biologically relevant metal ions, and high sensitivity. The sensing mechanism may be ascribed to the inhibited PET process from the coordination of Cr^{3+} and **1**. The '*in situ*' prepared Cr^{3+} complex (**1•Cr**) showed high selectivity and sensitivity (the LOD can be as low as 307 nM) toward S^{2-}, which can be used to sense S^{2-}. The lifetime of the sensor changes from 4.95 to 4.89 ns upon addition of Cr^{3+}, then the lifetime further increased to 5.88 ns upon addition of S^{2-} to the system above. In addition, the fluorescence and lifetime change of this chemosensor and the '*in situ*' prepared Cr^{3+} complex upon addition of Cr^{3+} and S^{2-} on test paper and in living cells have been successfully demonstrated.

Acknowledgements

We are grateful for the financial supports from National Natural Science Foundation of China (50903075 and J1210060), Key Laboratory of Photochemical Conversion and Optoelectronic Materials and Zhengzhou University.

References

[1] Lee MH, Kim JS, Sessler JL. Small molecule-based ratiometric fluorescence probes for cations, anions, and biomolecules. Chem Soc Rev 2015;44:4185−91.

[2] Carter KP, Young AM, Palmer AE. Fluorescent sensors for measuring metal ions in living systems. Chem Rev 2014;114:4564−601.

[3] Zhang X, Yin J, Yoon J. Recent advances in development of chiral fluorescent and colorimetric sensors. Chem Rev 2014;114:4918−59.

[4] Kim HN, Ren WX, Kim JS, Yoon J. Fluorescent and colorimetric sensors for detection of lead, cadmium, and mercury ions. Chem Soc Rev 2012;41:3210−44.

[5] Li Z, Yu M, Zhang L, Yu M, Liu J, Wei L, Zhang H. A "switching on" fluorescent chemodosimeter of selectivity to Zn^{2+} and its application to mcf-7 cells. Chem Commun 2010;46:7169−71.

[6] Wang J, Li Y, Patel NG, Zhang G, Zhou D, Pang Y. A single molecular probe for multi-analyte (Cr^{3+}, Al^{3+} and Fe^{3+}) detection in aqueous medium and its biological application. Chem Commun 2014;50:12258−61.

[7] Li X, Gao X, Shi W, Ma H. Design strategies for water-soluble small molecular chromogenic and fluorogenic probes. Chem Rev 2014;114:590−659.

[8] Sahoo SK, Sharma D, Bera RK, Crisponi G, Callan JF. Iron(iii) selective molecular

and supramolecular fluorescent probes. Chem Soc Rev 2012;41:7195−227.

[9] Mertz W. Chromium in human nutrition: A review. J Nutr 1993;123:626−33.

[10] Anderson RA. Chromium as an essential nutrient for humans. Regul toxicol pharmacol 1997;26:S35-41.

[11] Vincent JB. Recent advances in the nutritional biochemistry of trivalent chromium. Proc Nutr Soc 2004;63:41−7.

[12] Cervantes C, Campos-Garcia J, Devars S, Gutierrez-Corona F, Loza-Tavera H, Torres-Guzman JC, Moreno-Sanchez R. Interactions of chromium with microorganisms and plants. FEMS Microbiol Rev 2001;25:335−47.

[13] Eastmond DA, MacGregor JT, Slesinski RS. Trivalent chromium: Assessing the genotoxic risk of an essential trace element and widely used human and animal nutritional supplement. Crit Rev Toxicol 2008;38:173−90.

[14] Liu SH, Lu F, Zhu JJ. Highly fluorescent Ag nanoclusters: Microwave-assisted green synthesis and Cr^{3+} sensing. Chem Commun 2011;47:2661−3.

[15] Guo ZQ, Park S, Yoon J, Shin I. Recent progress in the development of near-infrared fluorescent probes for bioimaging applications. Chem Soc Rev 2014;43:16−29.

[16] Kubo K, Lloyd KG, Biddle JF, Amann R, Teske A, Knittel K. Archaea of the miscellaneous crenarchaeotal group are abundant, diverse and widespread in marine sediments. ISME J 2012;6:1949−65.

[17] Hou F, Huang L, Xi P, Cheng J, Zhao X, Xie G, Shi Y, Cheng F, Yao X, Bai D, Zeng Z. A retrievable and highly selective fluorescent probe for monitoring sulfide

and imaging in living cells. Inorg Chem 2012;51:2454−60.

[18] Nishida M, Sawa T, Kitajima N, Ono K, Inoue H, Ihara H, Motohashi H, Yamamoto M, Suematsu M, Kurose H, van der Vliet A, Freeman BA, Shibata T, Uchida K, Kumagai Y, Akaike T. Hydrogen sulfide anion regulates redox signaling via electrophile sulfhydration. Nat Chem Biol 2012;8:714−24.

[19] Zhu H, Fan J, Wang B, Peng X. Fluorescent, mri, and colorimetric chemical sensors for the first-row d-block metal ions. Chem Soc Rev 2015;44:4337−66.

[20] Shirinfar B, Ahmed N, Park YS, Cho GS, Youn IS, Han JK, Nam HG, Kim KS. Selective fluorescent detection of rna in living cells by using imidazolium-based cyclophane. J Am Chem Soc 2013;135:90−3.

[21] Lim NC, Pavlova SV, Bruckner C. Squaramide hydroxamate-based chemidosimeter responding to iron(iii) with a fluorescence intensity increase. Inorg Chem 2009;48:1173−82.

[22] Xu M, Wu S, Zeng F, Yu C. Cyclodextrin supramolecular complex as a water-soluble ratiometric sensor for ferric ion sensing. Langmuir 2010;26:4529−34.

[23] Weerasinghe AJ, Schmiesing C, Varaganti S, Ramakrishna G, Sinn E. Single- and multiphoton turn-on fluorescent Fe^{3+} sensors based on bis(rhodamine). J Phys Chem B 2010;114:9413−9.

[24] Goswami S, Aich K, Das S, Das AK, Sarkar D, Panja S, Mondal TK, Mukhopadhyay S. A red fluorescence 'off-on' molecular switch for selective detection of Al^{3+}, Fe^{3+} and Cr^{3+}: Experimental and theoretical studies along with living cell imaging. Chem Commun 2013;49:10739−41.

[25] Lu W, Zhou JT, Liu KY, Chen D, Jiang LM, Shen ZQ. A polymeric film probe with a turn-on fluorescence response to hydrogen sulfate ions in aqueous media. J Mater Chem B 2013;1:5014−20.

[26] Mahato P, Saha S, Suresh E, Di Liddo R, Parnigotto PP, Conconi MT, Kesharwani MK, Ganguly B, Das A. Ratiometric detection of Cr^{3+} and Hg^{2+} by a naphthalimide-rhodamine based fluorescent probe. Inorg Chem 2012;51:1769−77.

[27] Liu C, Pan J, Li S, Zhao Y, Wu LY, Berkman CE, Whorton AR, Xian M. Capture and visualization of hydrogen sulfide by a fluorescent probe. Angew Chem Int Ed 2011;50:10327−9.

[28] Choi MG, Cha S, Lee H, Jeon HL, Chang S-K. Sulfide-selective chemosignaling by a Cu^{2+} complex of dipicolylamine appended fluorescein. Chem Commun 2009:7390−2.

[29] Sasakura K, Hanaoka K, Shibuya N, Mikami Y, Kimura Y, Komatsu T, Ueno T, Terai T, Kimura H, Naganot T. Development of a highly selective fluorescence probe for hydrogen sulfide. J Am Chem Soc 2011;133:18003−5.

[30] Zhang L, Lou X, Yu Y, Qin J, Li Z. A new disubstituted polyacetylene bearing pyridine moieties: Convenient synthesis and sensitive chemosensor toward sulfide anion with high selectivity. Macromolecules 2011;44:5186−93.

[31] Cao X, Lin W, He L. A near-infrared fluorescence turn-on sensor for sulfide anions. Org Lett 2011;13:4716−9.

[32] Gu X, Liu C, Zhu Y-C, Zhu Y-Z. Development of a boron-dipyrromethene-Cu^{2+} ensemble based colorimetric probe toward hydrogen sulfide in aqueous media.

Tetrahedron Lett 2011;52:5000−3.

[33] Patnaik P. A Comprehensive Guide to the Hazardous Properties of Chemical Substances 3rd edn (New York: Wiley).

[34] Peng H, Cheng Y, Dai C, King AL, Predmore BL, Lefer DJ, Wang B. A fluorescent probe for fast and quantitative detection of hydrogen sulfide in blood. Angew Chem Int Ed 2011;50:9672−5.

[35] Yu F, Li P, Song P, Wang B, Zhao J, Han K. An ICT-based strategy to a colorimetric and ratiometric fluorescence probe for hydrogen sulfide in living cells. Chem Commun 2012;48:2852−4.

[36] Wang M-Q, Li K, Hou I-T, Wu M-Y, Huang Z, Yu X-Q. Binol-based fluorescent sensor for recognition of Cu(ii) and sulfide anion in water. J Org Chem 2012;77:8350−4.

[37] Hou X, Zeng F, Du F, Wu S. Carbon-dot-based fluorescent turn-on sensor for selectively detecting sulfide anions in totally aqueous media and imaging inside live cells. Nanotechnology 2013;24:335502.

[38] Wang T, Douglass EF, Jr., Fitzgerald KJ, Spiegel DA. A "turn-on" fluorescent sensor for methylglyoxal. J Am Chem Soc 2013;135:12429−33.

[39] Guha S, Lohar S, Banerjee A, Sahana A, Hauli I, Mukherjee SK, Sanmartin Matalobos J, Das D. Thiophene anchored coumarin derivative as a turn-on fluorescent probe for Cr^{3+}: Cell imaging and speciation studies. Talanta 2012;91:18−25.

[40] Mao J, Wang L, Dou W, Tang X, Yan Y, Liu W. Tuning the selectivity of two

chemosensors to Fe(iii) and Cr(iii). Org Lett 2007;9:4567−70.

[41] Wu H, Zhou P, Wang J, Zhao L, Duan C. Dansyl-based fluorescent chemosensors for selective responses of Cr(iii). New J Chem 2009;33:653−8.

[42] Liu D, Pang T, Ma K, Jiang W, Bao X. A new highly sensitive and selective fluorescence chemosensor for Cr^{3+} based on rhodamine b and a 4,13-diaza-18-crown 6-ether conjugate. RSC Adv 2014;4:2563−7.

[43] Xu Y, Yang W, Shao J, Zhou W, Zhu W, Xie J. A simple donor-acceptor probe for the detection of Cr^{3+} cations. RSC Adv 2014;4:15400−5.

[44] Wang J-N, Qi Q, Zhang L, Li S-H. Turn-on luminescent sensing of metal cations via quencher displacement: Rational design of a highly selective chemosensor for chromium(iii). Inorg Chem 2012;51:13103−7.

[45] Dang Y-Q, Li H-W, Wang B, Li L, Wu Y. Selective detection of trace Cr^{3+} in aqueous solution by using 5,5'-dithiobis (2-nitrobenzoic acid)-modified gold nanoparticles. ACS Appl Mater Inter 2009;1:1533−8.

[46] Zhang KY, Zhang J, Liu Y, Liu S, Zhang P, Zhao Q, Tang Y, Huang W. Core-shell structured phosphorescent nanoparticles for detection of exogenous and endogenous hypochlorite in live cells via ratiometric imaging and photoluminescence lifetime imaging microscopy. Chem Sci 2015;6:301−7.

[47] Zhao Q, Zhou X, Cao T, Zhang KY, Yang L, Liu S, Liang H, Yang H, Li F, Huang W. Fluorescent/phosphorescent dual-emissive conjugated polymer dots for hypoxia bioimaging. Chem Sci 2015;6:1825−31.

[48] Li M, Ge H, Arrowsmith RL, Mirabello V, Botchway SW, Zhu W, Pascu SI, James

TD. Ditopic boronic acid and imine-based naphthalimide fluorescence sensor for copper(ii). Chem Commun 2014;50:11806−9.

[49] Kaur A, Haghighatbin MA, Hogan CF, New EJ. A fret-based ratiometric redox probe for detecting oxidative stress by confocal microscopy, flim and flow cytometry. Chem Commun 2015;51:10510−3.

[50] Dmitriev RI, Borisov SM, Duessmann H, Sun S, Mueller BJ, Prehn J, Baklaushev VP, Klimant I, Papkovsky DB. Versatile conjugated polymer nanoparticles for high-resolution O-2 imaging in cells and 3d tissue models. ACS Nano 2015;9:5275−88.

[51] Wong CK, Laos AJ, Soeriyadi AH, Wiedenmann J, Curmi PMG, Gooding JJ, Marquis CP, Stenzel MH, Thordarson P. Polymersomes prepared from thermoresponsive fluorescent protein-polymer bioconjugates: Capture of and report on drug and protein payloads. Angew Chem Int Ed 2015;54:5317−22.

[52] Chen M, Wu Y, Liu Y, Yang H, Zhao Q, Li F. A phosphorescent iridium(iii) solvent complex for multiplex assays of cell death. Biomaterials 2014;35:8748−55.

[53] Bastiaens PI, Squire A. Fluorescence lifetime imaging microscopy: Spatial resolution of biochemical processes in the cell. Trends Cell Biol 1999;9:48−52.

[54] Berezin MY, Achilefu S. Fluorescence lifetime measurements and biological imaging. Chem Rev 2010;110:2641−84.

[55] Woo H, Cho S, Han Y, Chae W-S, Ahn D-R, You Y, Nam W. Synthetic control over photoinduced electron transfer in phosphorescence zinc sensors. J Am Chem Soc 2013;135:4771−87.

[56] Chen M, Lei Z, Feng W, Li C, Wang Q-M, Li F. A phosphorescent silver(i)-gold(i) cluster complex that specifically lights up the nucleolus of living cells with flim imaging. Biomaterials 2013;34:4284−95.

[57] Shi H, Sun H, Yang H, Liu S, Jenkins G, Feng W, Li F, Zhao Q, Liu B, Huang W. Cationic polyfluorenes with phosphorescent iridium(iii) complexes for time-resolved luminescent biosensing and fluorescence lifetime imaging. Adv Funct Mater 2013;23:3268−76.

[58] Lippert AR, New EJ, Chang CJ. Reaction-based fluorescent probes for selective imaging of hydrogen sulfide in living cells. J Am Chem Soc 2011;133:10078−80.

[59] Shao X, Kang R, Zhang Y, Huang Z, Peng F, Zhang J, Wang Y, Pan F, Zhang W, Zhao W. Highly selective and sensitive 1-amino bodipy-based red fluorescent probe for thiophenols with high off-to-on contrast ratio. Anal Chem 2015;87:399−405.

[60] Lee MH, Yoon B, Kim JS, Sessler JL. Naphthalimide trifluoroacetyl acetonate: A hydrazine-selective chemodosimetric sensor. Chem Sci 2013;4:4121−6.

[61] Du J, Hu M, Fan J, Peng X. Fluorescent chemodosimeters using "mild" chemical events for the detection of small anions and cations in biological and environmental media. Chem Soc Rev 2012;41:4511−35.

[62] Huang C, Jia T, Tang M, Yin Q, Zhu W, Zhang C, Yang Y, Jia N, Xu Y, Qian X. Selective and ratiometric fluorescent trapping and quantification of protein vicinal dithiols and in situ dynamic tracing in living cells. J Am Chem Soc 2014;136:14237−44.

[63] Lee MH, Park N, Yi C, Han JH, Hong JH, Kim KP, Kang DH, Sessler JL, Kang C,

Kim JS. Mitochondria-immobilized pH-sensitive off-on fluorescent probe. J Am Chem Soc 2014;136:14136−42.

[64] Lee MH, Jeon HM, Han JH, Park N, Kang C, Sesser JL, Kim JS. Toward a chemical marker for inflammatory disease: A fluorescent probe for membrane-localized thioredoxin. J Am Chem Soc 2014;136:8430−7.

[65] Du W, Xu J, Li H, Feng C, Yu M, Li Z, Wei L. Naked-eye and fluorescence detection of basic pH and F^- with a 1,8-naphthalimide-based multifunctional probe. RSC Adv 2015;5:15077−83.

[66] Liu X, Zhang W, Li C, Zhou W, Li Z, Yu M, Wei L. Nanomolar detection of hcy, GSH and cys in aqueous solution, test paper and living cells. RSC Adv 2015;5:4941−6.

[67] Li Z-X, Liao L-Y, Sun W, Xu C-H, Zhang C, Fang C-J, Yan C-H. Reconfigurable cascade circuit in a photo- and chemical-switchable fluorescent diarylethene derivative. J Phys Chem C 2008;112:5190−6.

[68] Yu D, Huang F, Ding S, Feng G. Near-infrared fluorescent probe for detection of thiophenols in water samples and living cells. Anal Chem 2014;86:8835−41.

[69] Liu Y, Li H, Pei M, Zhang G, Hu L, Han J. A new fluorescence "off-on" chemodosimeter for l-cysteine based on water-soluble polythiophene. Talanta 2013;115:190−4.

Figure Captions

Scheme 1 Synthetic route to sensor **1**.

Fig. 1. Emission spectra of **1** (1.0×10^{-5} M, V_{water}:$V_{ethanol}$ = 6:4) upon titration of Cr^{3+} water solution (0–33 equiv to **1**) with excitation at 385 nm. The linearity of peak intensity with respect to Cr^{3+} concentrations (right).

Fig. 2. Fluorescence spectra (up) and photographs (down) of **1** (1.0×10^{-5} M, V_{water}:$V_{ethanol}$ = 6:4) upon addition of 2 equiv. various metal ions with excitation at 385 nm (up) and under a 365 nm UV lamp (down). The metal ions used from left to right were only **1**, K^+, Ca^{2+}, Na^+, Mg^{2+}, Al^{3+}, Zn^{2+}, Co^{2+}, Ni^{2+}, Pb^{2+}, Cu^{2+}, Cr^{3+}, Hg^{2+}, Mn^{2+} and Cd^{2+}.

Fig. 3. Fluorescence responses of **1** (1.0×10^{-5} M, V_{water}:$V_{ethanol}$ = 6:4) upon addition of 10 equiv different metal ions (black bars), and fluorescence changes of the mixture of **1** and 3 equiv. Cr^{3+} after addition of 10 equiv metal ions (red bars). The excitation wavelength was 385 nm. I_0 represents the emission intensity at 520 nm in the fluorescence spectroscopy of compound **1**. I represents the emission intensity at 520 nm in the fluorescence spectroscopy of compound **1** after addition of the species to the solution of **1** (black bars) and of the mixture of **1** and Cr^{3+} after addition of an excess of the species (red bars). The metal ions used were only **1**, Cr^{3+}, K^+, Ca^{2+}, Na^+, Mg^{2+}, Al^{3+}, Zn^{2+}, Co^{2+}, Ni^{2+}, Pb^{2+}, Cu^{2+}, Hg^{2+}, Mn^{2+}, and Cd^{2+}.

Fig. 4. Emission spectra of the '*in situ*' prepared complex **1•Cr^{3+}** (1.0×10^{-5} M, water/ethanol = 6:4, v/v) in the presence of S^{2-} water solution (left). Emission spectra response of the '*in situ*' prepared complex **1•Cr^{3+}** at 520 nm as a linear dependence with the concentration of S^{2-} (right).

Fig. 5. Fluorescence emission spectra response of the '*in situ*' prepared complex

1•Cr^{3+} (1.0 × 10^{-5} M, water/ethanol = 6:4, v/v) at 520 nm in the presence of different anions (4.0 × 10^{-5} M) (black bars) and fluorescence emission spectra response of the '*in situ*' prepared complex **1•Cr^{3+}** (1.0 × 10^{-5} M, water/ethanol = 6:4, v/v) and S^{2-} (4.0 × 10^{-5} M) after addition of other different anions (4.0 × 10^{-5} M) (red bars). The anions from 1 to 20 are only **1**, S^{2-}, F^-, Cl^-, Br^-, I^-, CO_3^{2-}, CH_3COO^-, NO_3^-, PO_4^{3-}, NO_2^-, SO_3^{2-}, HSO_3^-, ClO_3^-, N_3^-, SiO_3^{2-}, HCO_3^-, HPO_4^{2-}, $H_2PO_4^-$, SCN^-, and SO_4^{2-}.

Fig. 6. (a) Fluorescence spectra and (b) fluorescence intensity at 495 nm of the sensor spots of **1** (1.0 × 10^{-5} M, water/ethanol = 6:4, v/v) on test papers upon addition of various concentrations of Cr^{3+} (0–10 mM).

Fig. 7. Images of test papers for the selectivity of Cr^{3+} upon addition of 10 mM various metal ions (From left to right, the metal ions used were only **1**, K^+, Ca^{2+}, Na^+, Mg^{2+}, Al^{3+}, Zn^{2+}, Co^{2+}, Ni^{2+}, Pb^{2+}, Cu^{2+}, Cr^{3+}, Hg^{2+}, Mn^{2+} and Cd^{2+}) under a UV lamp (365 nm).

Fig. 8. Confocal fluorescence contrast images of living hela incubated with 10 μM sensor **1** at 37 °C for 10 min (a and d), incubated with 10 μM sensor **1** and 40 μM Cr^{3+} at 37 °C for 5 min (b and e), and incubated with 10 μM sensor **1**, 40 μM Cr^{3+} and 80 μM S^{2-} at 37 °C for 2 min (c and f).

Fig. 9. FLIM images in live hela cells constained by 10 μM sensor **1** (a), cells pretreated with 10 μM sensor **1** followed by incubation with 40 μM Cr^{3+} (b), and incubated with 10 μM sensor **1**, 40 μM Cr^{3+} and 80 μM S^{2-} (c).

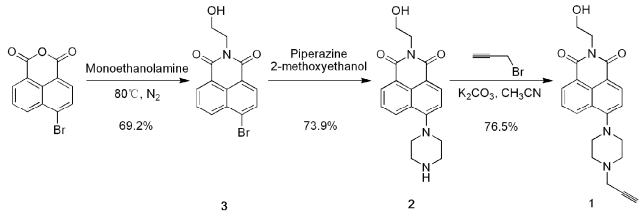

Scheme 1 Synthetic route to sensor **1**.

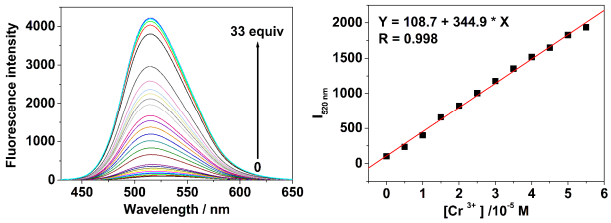

Fig. 1. Emission spectra of **1** (1.0×10^{-5} M, V_{water}:$V_{ethanol}$ = 6:4) upon titration of Cr^{3+} water solution (0–33 equiv to **1**) with excitation at 385 nm. The linearity of peak intensity with respect to Cr^{3+} concentrations (right).

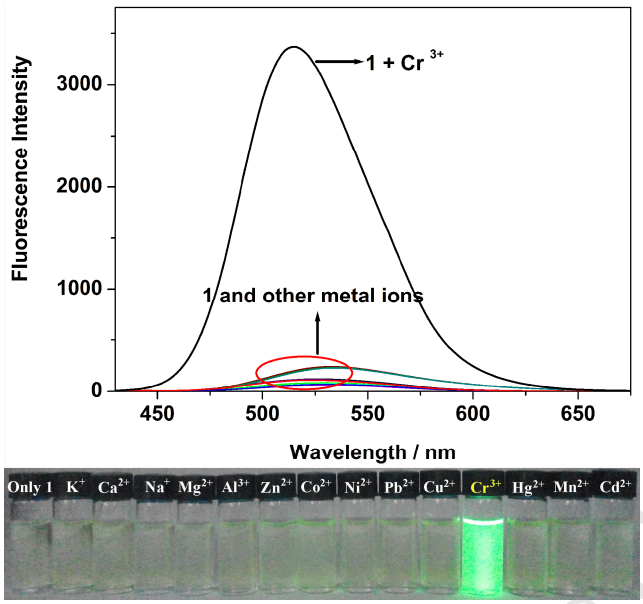

Fig. 2. Fluorescence spectra (up) and photographs (down) of **1** (1.0×10^{-5} M, V_{water}:$V_{ethanol}$ = 6:4) upon addition of 2 equiv. various metal ions with excitation at 385 nm (up) and under a 365 nm UV lamp (down). The metal ions used from left to right were only **1**, K^+, Ca^{2+}, Na^+, Mg^{2+}, Al^{3+}, Zn^{2+}, Co^{2+}, Ni^{2+}, Pb^{2+}, Cu^{2+}, Cr^{3+}, Hg^{2+}, Mn^{2+} and Cd^{2+}.

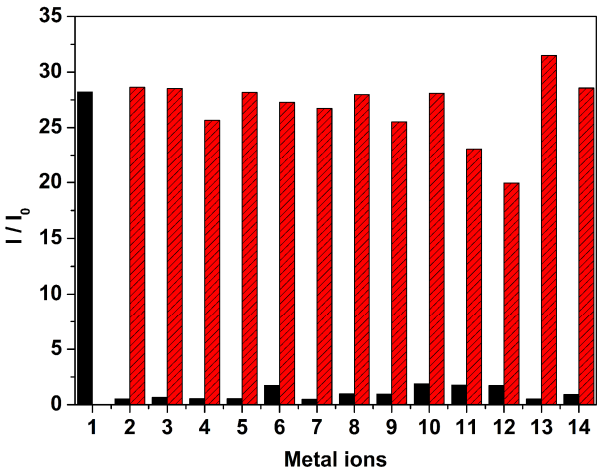

Fig. 3. Fluorescence responses of **1** (1.0×10^{-5} M, V_{water}:$V_{ethanol}$ = 6:4) upon addition of 10 equiv different metal ions (black bars), and fluorescence changes of the mixture of **1** and 3 equiv. Cr^{3+} after addition of 10 equiv metal ions (red bars). The excitation wavelength was 385 nm. I_0 represents the emission intensity at 520 nm in the fluorescence spectroscopy of compound **1**. I represents the emission intensity at 520 nm in the fluorescence spectroscopy of compound **1** after addition of the species to the solution of **1** (black bars) and of the mixture of **1** and Cr^{3+} after addition of an excess of the species (red bars). The metal ions used were only **1**, Cr^{3+}, K^{+}, Ca^{2+}, Na^{+}, Mg^{2+}, Al^{3+}, Zn^{2+}, Co^{2+}, Ni^{2+}, Pb^{2+}, Cu^{2+}, Hg^{2+}, Mn^{2+}, and Cd^{2+}.

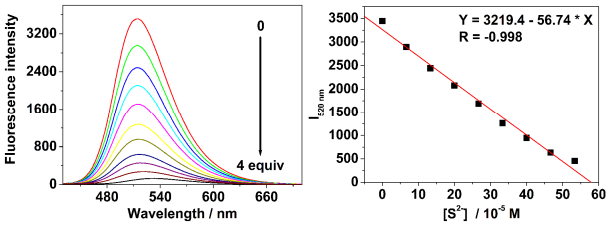

Fig. 4. Emission spectra of the '*in situ*' prepared complex **1•Cr**$^{3+}$ (1.0 × 10^{-5} M, water/ethanol = 6:4, v/v) in the presence of S^{2-} water solution (left). Emission spectra response of the '*in situ*' prepared complex **1•Cr**$^{3+}$ at 520 nm as a linear dependence with the concentration of S^{2-} (right).

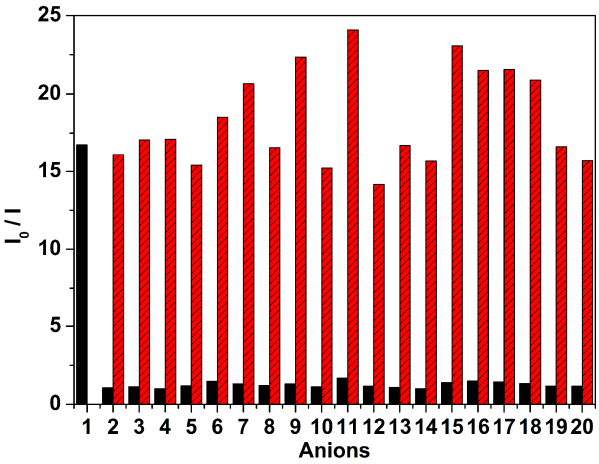

Fig. 5. Fluorescence emission spectra response of the '*in situ*' prepared complex **1•Cr**$^{3+}$ (1.0×10^{-5} M, water/ethanol = 6:4, v/v) at 520 nm in the presence of different anions (4.0×10^{-5} M) (black bars) and fluorescence emission spectra response of the '*in situ*' prepared complex **1•Cr**$^{3+}$ (1.0×10^{-5} M, water/ethanol = 6:4, v/v) and S^{2-} (4.0×10^{-5} M) after addition of other different anions (4.0×10^{-5} M) (red bars). The anions from 1 to 20 are only **1**, S^{2-}, F^-, Cl^-, Br^-, I^-, CO_3^{2-}, CH_3COO^-, NO_3^-, PO_4^{3-}, NO_2^-, SO_3^{2-}, HSO_3^-, ClO_3^-, N_3^-, SiO_3^{2-}, HCO_3^-, HPO_4^{2-}, $H_2PO_4^-$, SCN^-, and SO_4^{2-}.

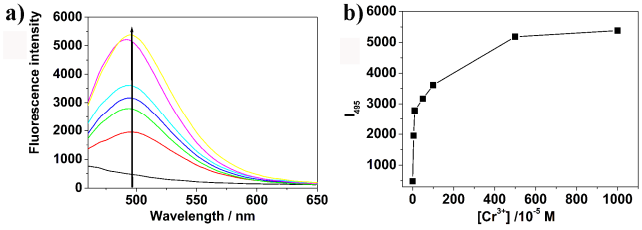

Fig. 6. (a) Fluorescence spectra and (b) fluorescence intensity at 495 nm of the sensor spots of **1** (1.0×10^{-5} M, water/ethanol = 6:4, v/v) on test papers upon addition of various concentrations of Cr^{3+} (0–10 mM).

Fig. 7. Images of test papers for the selectivity of Cr^{3+} upon addition of 10 mM various metal ions (From left to right, the metal ions used were only **1**, K^{+}, Ca^{2+}, Na^{+}, Mg^{2+}, Al^{3+}, Zn^{2+}, Co^{2+}, Ni^{2+}, Pb^{2+}, Cu^{2+}, Cr^{3+}, Hg^{2+}, Mn^{2+} and Cd^{2+}) under a UV lamp (365 nm).

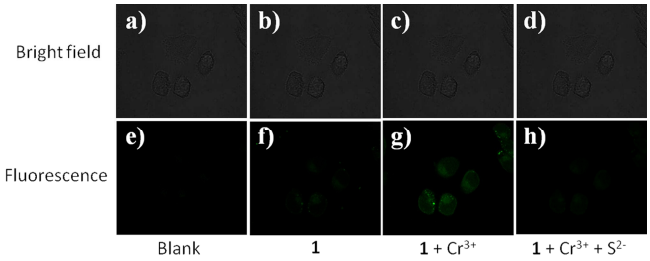

Fig. 8. Confocal fluorescence contrast images of living hela incubated with 10 μM sensor **1** at 37 °C for 10 min (a and d), incubated with 10 μM sensor **1** and 40 μM Cr^{3+} at 37 °C for 5 min (b and e), and incubated with 10 μM sensor **1**, 40 μM Cr^{3+} and 80 μM S^{2-} at 37 °C for 2 min (c and f).

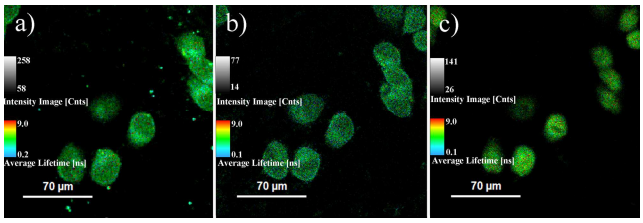

Fig. 9. FLIM images in live hela cells constained by 10 μM sensor **1** (a), cells pretreated with 10 μM sensor **1** followed by incubation with 40 μM Cr^{3+} (b), and incubated with 10 μM sensor **1**, 40 μM Cr^{3+} and 80 μM S^{2-} (c).

Highlights

►A Cr^{3+} selective fluorescent "off-on" and lifetime-based chemosensor was synthesized.

►The chemosensor was capable of quantitatively detect the concentration of Cr^{3+} by a dramatically enhanced fluorescence.

►The '*in situ*' prepared Cr^{3+} complex showed high selectivity and sensitivity toward S^{2-}.

►The calculated low detection limit (LOD) value is as low as 307 nM for S^{2-}.

►The lifetime changed from 4.95 to 4.89 ns upon the addition of Cr^{3+}, and further increased to 5.88 ns upon addition of S^{2-}.